Comparison of Simple and B_1-Compensated Spin-Lock Preparation Techniques at Strong B_0 Magnetic Field Inhomogeneities

P. Martirosian[1], M. Deimling[2], B. Kiefer[2], N. F. Schwenzer[1,3], and F. Schick[1]

[1]Section on Experimental Radiology, University of Tübingen, Tübingen, Germany, [2]Siemens Medical Solutions, Erlangen, Germany, [3]Department of Diagnostic Radiology, University of Tübingen, Tübingen, Germany

Purpose

Spin-lock (SL) techniques are promising for improving contrast and tissue characterization in MR imaging regarding cartilage diseases by exploiting the relaxation time $T1_\rho$, the spin-lattice relaxation time in the rotating frame of reference[1-3]. An essential improvement of image quality in SL technique was achieved by the development of a B_1-insensitive SL pulse[4]. The idea of this SL pulse is based on the so-called rotary echo technique and corrects image artifacts due to the field inhomogeneity of the RF transmit coil[5]. The purpose of this work was the theoretical and experimental comparison between a simple (B_1-non-compensated) SL technique and the B_1-compensated SL preparation at strong static magnetic field inhomogeneities.

Materials and Methods

Theory: In a basic SL experiment, the equilibrium longitudinal magnetization $\mathbf{M_0}$ is tilted to the transverse plane by a 90° RF pulse. This is followed immediately by a locking RF pulse, $\mathbf{B}_{SL}$, which is applied during the locking time T_{SL}. The phase of $\mathbf{B}_{SL}$ is adjusted to be parallel aligned with the tilted magnetization vector $\mathbf{M}$. In general, the locked magnetization decays under the influence of relaxation with a time constant $T_{1\rho}$. The problem in the basic SL experiment is that in the presence of an inhomogeneous $\mathbf{B}_{SL}$, the magnetization vectors from spins in various parts of the sample fan out as they precess in the *yz*-plane. The rotary-echo SL experiment eliminates this problem in similar way as the spin echo technique overcomes inhomogeneity effects in B_0: at the time τ after application of the RF field, its phase is changed by 180° as it is shown in Fig. 1a. Those spins that experience the largest $\mathbf{B}_{SL}$, hence have precessed farthest, now precess fastest in the opposite direction. However, there is possible dephasing due to local magnetic field inhomogeneities $\mathbf{B}_{loc}$. Therefore the motion of the vector $\mathbf{M}$ follows a cone of precession about an effective field $\mathbf{B}_{eff} = \mathbf{B}_{loc}+\mathbf{B}_{SL}$, which makes an angle $\theta = \tan^{-1}(B_{SL}/B_{loc})$ with the z axis (Fig. 1b). In this case, the 180°-phase switch does not correct compensate B_1-inhomogeneities. The behavior of the spin magnetization $\mathbf{M}$ can be described in a non-tilted frame by the rotating matrix formalism. M_x and M_y describe the movement (generally elliptical) of the transverse magnetization vector $\mathbf{M}_\perp$ in the *xy*-plane. The angle ϕ between $\mathbf{M}_\perp$ and *y*-axis specifies the dephasing degree of the transverse magnetization[6].

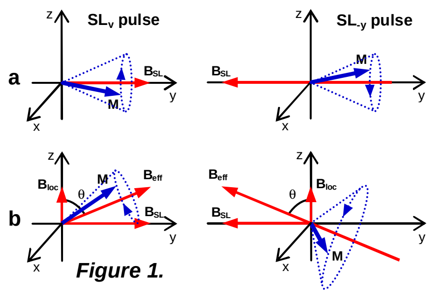

Figure 1.

Experiment: Measurements were performed on a 1.5 T whole-body MR scanner (Siemens Medical Solutions, Erlangen, Germany). The circular polarized transmit/receive extremity coil was used. Measurements at a homogeneous cylindrical water phantom were performed using a SL prepared sequence. In the measurements with simple SL pulse, the longitudinal magnetization was prepared by a non-selective RF pulse train $90°_x$ - SL_y - $90°_{-x}$ (Fig. 2a). The SL pulse length T_{SL} was 60 ms and the amplitude B_{SL} was varied between 0 µT and 11.8 µT. The SL pulse in rotary-echo SL experiments (Fig. 2b) consisted of two identical pulses SL_y and SL_{-y} with duration of $T_{SL}/2$ and a relative phase shift of 180° from each other. Immediately after the restoring pulse, the residual transverse component was spoiled. The prepared magnetization was excited and acquired with a single-shot RF-spoiled gradient echo sequence (FLASH) with following parameters: TR = 2.8 ms, TE = 1.4 ms, flip angle = 8°, slice thickness = 5 mm, FoV = 200×200 mm^2, matrix = 64×64, BW = 490 Hz/pixel. Macroscopic field inhomogeneities were generated by using the shimming coil of the scanner: an additional linear gradient ΔG_R = 20 µT/m was applied along the read-out direction.

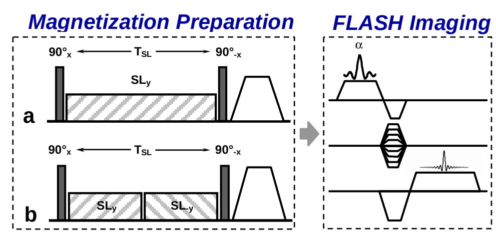

Figure 2.

Results

Figure 3 shows the calculated dephasing angle function ϕ in dependence of T_{SL} for B_{SL} = 3, 6, and 12 µT at B_{loc} = 1 µT. It is obvious that the maximal dephasing angle ϕ_{max} of the transverse magnetization suddenly increases at the switch time of the second SL pulse and that its value is mainly influenced by the ratio B_{SL}/B_{loc}. Effects of the simple and the rotary-echo SL pulse on transverse magnetisation in the presence of B_1 field inhomogeneities for varied B_{SL} are shown in Fig. 4a and 4b. Results show that the rotary-echo technique leads to the compensation of B_1-inhomogeneity of the transmit coil, which is clearly visible on the images with the simple SL. However, this compensation is only effective at a B_{SL} from 11.8 µT down to 0.75 µT (red arrow). For values lower than 0.75 µT, images obtained with the rotary-echo SL pulse show much more artifacts (green arrow). This effect is even more pronounced, if the additional linear gradient ΔG_R artificially enhances the static magnetic field inhomogeneities. In this case, images obtained with rotary-echo technique showed stronger artifacts even at B_{SL} = 11.8 µT (Fig. 4c and 4d).

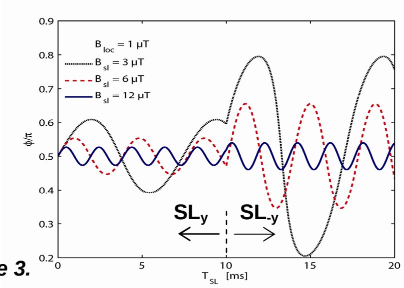

Figure 3.

Discussion

The presented results demonstrate that the rotary-echo SL pulse compensates B_1-inhomogeneity of the transmit coil. However, this technique has only an advantageous compared to the simple SL pulse, if the SL amplitude is much higher then static local field inhomogeneities.

For this reason, the simple SL pulse is suitable for the acquisition of artifacts-free images in body regions with strong static B_0-field inhomogeneities due to susceptibility changes in tissues (especially in trabecular bone and in regions adjacent to air containing cavities).

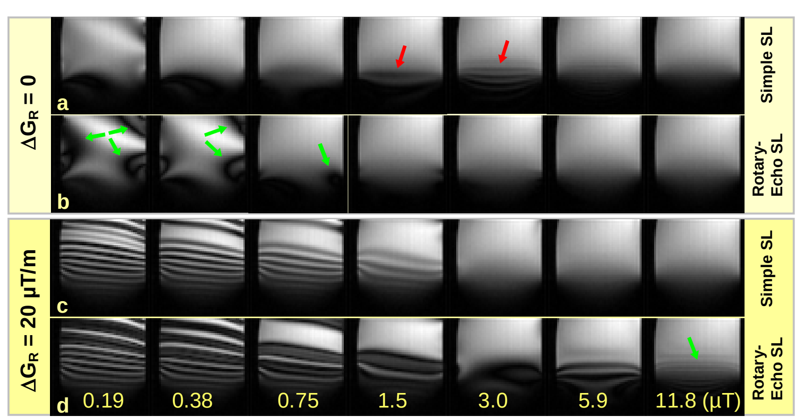

Figure 4.

References

1. Aronen HJ. MRI 1999;17:1001-10.
2. Wheaton AJ. JMRI 2004;20:519-25.
3. Pakin SK. MRM 2007;56:561-73.
4. Charagundla SR et al. J Magn Reson 2003;162:113–21.
5. Solomon I. Phys Rev Lett 1959;2:301-02.
6. Martirosian P et al. In Proc ISMRM 2001, p. 856.